Influence of dynamic parameters on interacting efficiency between ground-based laser and air-based flying target

Shaoyong Deng (邓少永)*, Shiqiang Zhang (张世强), Yanhong Sun (孙艳宏), and Xiaowei Guan (关小伟)

Northwest Institute of Nuclear Technology, Xian710024, China

**Corresponding author: sydeng_2004@163.com*

Received January 15, 2014; accepted March 15, 2014; posted online November 3, 2014

We simulate the integrated effects of atmospheric aberration, atmospheric turbulence, thermal blooming, random jitter of laser's intensity and phase, speed of wind, direction of wind, absorption of air, kinetic cooling of CO_2 and N_2, speed of target, output power and beam quality of laser, wavelength, focus length, and the launch altitude of laser to accurately simulate the transmission loss of the laser's energy, concentration of laser's power and other beam quality parameters of the laser propagating to the dynamic target. And we evaluate the efficiency of laser's irradiation on the target more accurately for the optical link of ground-to-airspace. We also investigate influences of characteristics of dynamic parameters (Strehl's ratio, RMS of wavefront, spatial distribution of intensity on the target, the real focus on the optical link and the peak intensity along the propagation path) including speed of wind, direction of wind, speed of target and the kinetic cooling effect of air, especially. We conclude that the higher speed of wind and target weakens the thermal blooming of atmosphere and improves the beam quality and efficiency of laser's irradiation on the target. The kinetic cooling effect of air is more remarkable to improve the beam quality irradiating on the target at the initial part of the propagation path of the laser. The changed direction of wind weakens the atmospheric aberration and directs to better beam quality and higher efficiency of laser's irradiation on the target.

OCIS codes: 010.1290, 010.1300, 010.1330.

doi: 10.3788/COL201412.S20101.

With improvements in laser power and beam quality control technology, the adaptive filtering and control methods for wavefront prediction and correction, and precise pointing laser beams to compensate for the atmospheric turbulence, thermal blooming, platform vibration, target motion and sensor noise degrade the performance of the optical link of laser to target[1]. We should investigate the characteristics of the ground–space and ground–airspace optical links to learn how to improve the efficiency of laser's irradiation on the target. The atmospheric aberrations on the propagation path are studied for different kinds of laser[2] through different simplified models and some integrated influences of atmospheric propagation are ignored. All studied on this have shown abounding results; however, the simplification of simulation models could not evaluate the efficiency of laser's irradiation on the target accurately.

It is well known that the efficiency of laser's irradiation on the target is influenced by the integrated effects of atmospheric aberration, atmospheric turbulence, thermal blooming, random jitter of laser's intensity and phase, speed of wind, direction of wind, absorption and scattering of air, kinetic cooling of CO_2 and N_2, speed of target, output power and beam quality of laser, wavelength and launch altitude of laser. We will investigate all these influencing parameters to accurately simulate the transmission loss of the laser's energy, concentration of laser's power and other beam quality parameters of the laser propagating to the dynamic target, and we will also evaluate the efficiency of laser's irradiation on the target more accurately based on the optical link of ground to airspace[3,4].

We used the CO_2 laser with a wavelength is 10.6 μm. It is well known that the CO_2 laser is the ideal source to be used in the laser propulsion. The system of laser propulsion deals with the influences of atmospheric propagation characteristics on ground-based laser system, the light craft of relay system and the target of macrosatellite[5].

Under proper conditions, the CO_2 laser beam may cause kinetic cooling, which occurs as a transient condition when the CO_2 absorption in the atmosphere is significant. According to Smith[6], as the CO_2 molecule absorbs radiation in going from the (1000) state to (0001) state, energy is absorbed from the vibrational (1000) level. Consequently, (1000) is no longer in thermal equilibrium and the state is repopulated quickly by taking energy out of the translational energy reservoir. This process results in an immediate drop in temperature. Ultimately, the energy in the (0001) state is distributed into the first vibrational state of nitrogen. The excited nitrogen atoms decay slowly through any of the available routes, so that for some modest period of time, the effect of the laser is to cool the gas.

Here we investigate the integrated influences of atmospheric aberration on absorption of vapor, CO_2, aerosol, etc., atmospheric turbulence, thermal bloom, random jitter of laser's intensity and phase, altitude of laser's launch system, speed and direction of wind, speed of target, focus of laser launch system and the kinetic cooling of CO_2 and N_2 on the transmission path

of laser. The numerical solutions show the influences of atmospheric link to the beam quality and the efficiency of laser's irradiation on the dynamic target at airspace.

We used GLAD software for simulation[7]. The atmospheric aberration is described by Kolmogorov spectral distribution. The jitter of laser is simulated by the random tilt and phase. It is assumed that scattering plays a negligible role. In simple form, the temperature rise ΔT due to absorption is calculated as

$$\Delta T = \frac{a}{\rho C}\int_{-\infty}^{0} I(\tau)\,d\tau, \tag{1}$$

where α is the loss coefficient due to absorption by water vapor, CO_2, and other components of the atmosphere, ρ is the density of atmosphere, $I(\tau)$ is the intensity of laser, C is the absolute specific heat, and τ is the irradiation time.

$$I(x,y,\tau) = I\left(x-\Delta x(\tau), y-\Delta y(\tau)\right). \tag{2}$$

The spatial shifts $\Delta x(\tau)$ and $\Delta y(\tau)$ are defined as

$$\Delta x(\tau) = \left[v_{w_x} + \frac{s}{s_t} v_{t_x}\right]\tau = v_{c_x}\tau, \tag{3}$$

$$\Delta y(\tau) = \left[v_{w_y} + \frac{s}{s_t} v_{t_y}\right]\tau = v_{c_y}\tau, \tag{4}$$

where v_{c_x} and v_{c_y} are net components of velocity, v_{w_x} and v_{w_y} are components of wind velocity, v_{t_x} and v_{t_y} are components of target velocity, S is slant range of the current beam position, and s_t is slant range of the target. For sufficient short intervals of Δz along the optical path, the slant range does not vary significantly and the velocity components may be considered constant over that interval. As shown above, the temperature is based on the time integration of the beam moving in atmosphere. We may disregard the times sufficiently far back that no part of the beam overlaps the position of interest. The number of sample array is N and the sample space is Δx, the relationship of speed v with time τ_{trans} for the atmosphere to sweep past the beam due to the combined effects of beam steering and wind is shown as:

$$\tau_{\text{trans}} \approx \frac{N\Delta x}{v}. \tag{5}$$

The temperature rise can be rewritten as

$$\Delta T(x,y) = -\frac{a}{\rho C}\int_{-\infty}^{0} I\left(x - v_{c_x}\tau, y - v_{c_y}\tau\right)d\tau. \tag{6}$$

The heating of the atmosphere causes the gas to expand at constant pressure. The expansion takes place at the rate of the sound propagation in the air. As the volume increases, the density drops proportionally. The equation for index change is given by

$$\Delta n = -(n_0 - 1)\frac{P_{\text{rel}}}{T_{\text{rel}}}\frac{\Delta T}{T}, \tag{7}$$

where P_{rel} is the relative atmospheric pressure, T_{rel} is the relative temperature with respect to standard temperature and pressure (STP), T is the temperature at some altitude, and n_0 is the index of refraction at STP.

The phase aberration on the propagation step length Δz is given as

$$\phi = -\frac{2\pi}{\lambda}(n_0 - 1)\frac{P_{\text{rel}}}{T_{\text{rel}}}\frac{\Delta T}{T}\Delta z. \tag{8}$$

The propagation link over water area is ignored and the influence of humidity is slightly than 1%. The refractive index is the function of wavelength of λ, temperature T and pressure P[2]:

$$n = 1 + 77.6\times\left(1 + 7.52\times10^{-3}\lambda^{-2}\right)\frac{P}{T}\times10^{-8}. \tag{9}$$

The temperature T and pressure P are decided by altitude. The unit of λ is μm, and T_0 is the temperature at sea level. At standard pressure and at sea level, $T_0 = 288.15$ K, and $P_0 = 1.01325\times10^5$ Pa, $h_a = 11$ km, $h_b = 22$ km, and $\Delta_1 = -6.5$ K/km. All the parameters of atmosphere on propagation length are based on US Standard Atmosphere 1976.

Given the altitude, the code will calculate the temperature, pressure, index of refraction and absorption of the atmosphere. The absorption of N and CO_2 is broken out separately to enable the effects of kinetic cooling to be included. The effect may be important if the beam is crossing through the air very rapidly. The effect may reduce or reverse the thermal defocusing of the atmosphere. The user may also explicitly define the atmospheric parameters rather than using the values calculated using GLAD.

The attenuation effects of the atmosphere as well as the phase perturbations due to temperature change in the air are included. The relative rate at which the beam crosses through the air due to wind and beam steering may be specified. The phase change causes the beam to change its degree of convergence, direction and amount of aberration. The code will test for excessive growth of the beam within the bounds of the computer array and automatically rescales and recenters the beam as required.

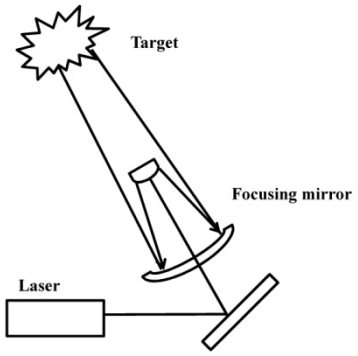

Fig. 1. Optical link for numerical simulations.

Figure 1 shows optical link for numerical simulations. The parameters for simulation are characterized as follows: wavelength is 10.6 μm, the altitude to launch laser is 1 km, the temperature is 281.65 K, the pressure is 0.89875e5 Pa, the relative temperature is 0.977, the relative pressure is 0.887, the refractive index is 1.000248, the beam radius of laser is 25 cm, the distance between the laser system and target in the air base is 4 km, the atmospheric coherent length for 4 km propagation path is 10 cm. The propagation path of laser is separated by 40 steps and the atmospheric coherent length for every step of length is $r = 10\times40^{3/5} = 92$ cm. The absorption coefficient of aerosol is 4.365×10^{-3}/km, the absorption coefficient of vapor is 1.0×10^{-3}/km, and the absorption coefficient of CO_2 is 3.0×10^{-2}/km. The conductivity is 0.02525 W/mK, the specific heat is 1017 J/kg K, and the density of atmosphere is 1.116 kg/m^3. The wind speed is (−10, −10) m/s at the first propagation length of 2 km and the wind speed would change to (−10, 10) m/s at the last 2 km of propagation length. The target velocity is (4, −4) m/s.

The Strehl ratio is used to evaluate the beam quality and it is convenient to use a modified version of the ratio of the center of the far-field intensity with aberration to the far-field intensity with no aberrations.

$$\text{Strehl's ratio} = \frac{I(0,0)_{\text{aber}}}{I(0,0)_{\text{noaber}}}. \tag{10}$$

The evaluations of beam quality and action efficiency of high-power laser focus on the power in bucket on the target of far field.

The discrepancy of maximum phase of the adjacent sample gridding is less than π, therefore, the sample spacing should satisfy following relationship:

$$\frac{\lambda z}{4D} < \Delta x < \frac{\pi^{\frac{3}{2}} D}{N_D}. \tag{11}$$

The propagation step of Δz should satisfy the relationship of $\Delta z < 4D\Delta x/\lambda$. The magnitude of Δx Δx is 10^{-3} – 10^{-2} m and the magnitude of Δz is 10^2 – 10^4 m. Here, the Δx is 2.5 cm and Δz is 1 km.

Since a typical value for the nitrogen decay time constant is $\tau_{N_2} = 0.015$ s, the kinetic cooling may be a factor if the beam crossing time is less than the nitrogen decay time:

$$\frac{\tau}{\tau_{N_2}} \ll 1. \tag{12}$$

This condition may occur for fast beam steering resulting in cancellation or reversal of the usual kinetic heating effect. Kinetic cooling is incorporated by Hogge into the equations as

$$\sigma = 2.441(n_0 - 1)\frac{a_{CO_2}}{a}, \tag{13}$$

where σ is a kinetic cooling factor. The complete equation of temperature rise including kinetic cooling is

$$\Delta T(x,y) = -\frac{a}{\rho C}\int_{-\infty}^{0}\left(1 - \sigma e^{-\frac{\tau}{\tau_{N_2}}}\right) I\left(x - v_{c_x}\tau, y - v_{c_y}\tau\right) d\tau. \tag{14}$$

The integral over time may be accomplished by performing a moving average over the irradiance distribution. For general components, this requires an interpolation step across matrix lines which are numerically noisy. When kinetic cooling is negligible, a particularly smooth way to do this is to calculate the moving average by integrating in the frequency domain.

The peak intensity of laser is 500 W/cm^2 and three different conditions are investigated here. The first condition is to ignore the kinetic cooling of CO_2 and N_2, the second condition is to consider the kinetic cooling on the last 2 km propagation path, the third condition is to consider the kinetic cooling on the whole propagation path. The Strehl ratio, RMS of wavefront, peak intensity and the power on target of the three conditions are shown in Table 1. The Strehl ratio shows the characteristics of the high-power laser at far field. The peak intensity and power show the characteristics of the high-power laser at near field.

Figure 2 shows spatial distributions of the high-power laser's intensity at near field for different propagation lengths of 0 and 2 km. The original laser is the standard Gaussian beam at 0 km as shown in Fig. 2(a). It is seen that the thermal blooming of atmosphere would be remarkable if the kinetic cooling effect is ignored as shown in Fig. 2(b). The kinetic cooling effect of CO_2 and N_2 would weaken the thermal blooming of atmosphere as shown in Fig. 2(c).

Table 1 shows that the numerical results are very close for ignoring kinetic cooling and considering kinetic cooling only for the last 2 km of propagation path.

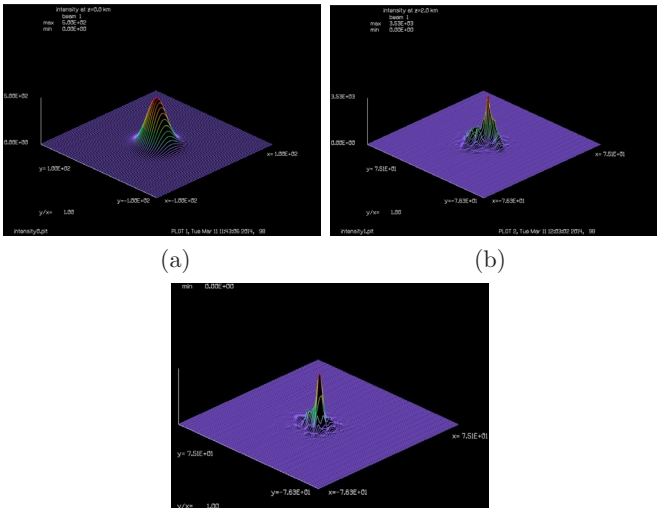

(a) (b)

(c)

Fig. 2. Intensity distributions of (a) the original laser at 0 km, (b) 2 km of ignoring kinetic cooling, and (c) 2 km considering kinetic cooling.

Table 1. Evaluation Parameters of the Dynamic Target

Kinetic Cooling	Strehl's Ratio	RMS w.f. Waves	Peak Intensity(W/cm²)	Power(W)
Uncooled	0.0020	0.396	1150	391886
Half Cooled	0.0020	0.396	1150	391889
Totally Cooled	0.0023	0.392	1780	391888

Influences of kinetic cooling of the first 2 km on the propagation path are remarkable for the beam quality (Strehl's ratio and RMS of wavefront) and efficiency of irradiation (peak intensity and power) on the dynamic target. It should be considered for the higher absorption coefficient of atmosphere. The kinetic parameter σ is higher for the higher α_{CO_2} and thermal bloom on the first 2 km of propagation path is weakened. As high-power laser propagates to the target, α_{CO_2} becomes lower; therefore, the kinetic cooling becomes weaker and could not weaken the thermal blooming of atmosphere.

Figure 3 shows the spatial distribution of laser intensity on the target corresponding to three different simulation conditions. Figure 4 shows the peak intensity and the real focus of the laser on the propagation link. It should be observed that the position of the real focus will change for the kinetic cooling of CO_2 and N_2 on the optical link and the evaluation of the laser's irradiation efficiency will be influenced. Figure 3 shows

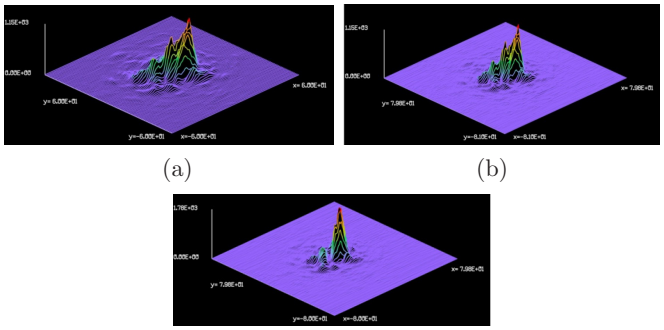

(a) (b)

(c)

Fig. 3. (a) Intensity distribution on the target for conditions of ignoring kinetic cooling, (b) considering kinetic cooling on the last 2 km propagation path, and (c) and considering the kinetic cooling on the whole propagation path.

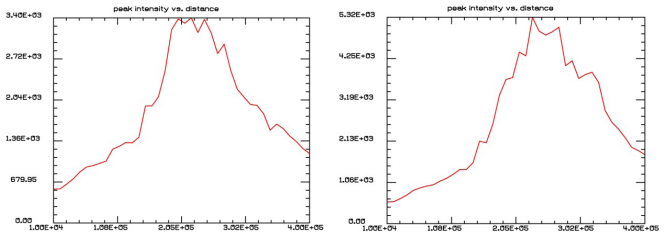

(a) (b)

Fig. 4. Peak intensity on the optical path for conditions of considering kinetic cooling on (a) the last 2 km propagation path and (b) the whole propagation path.

that the spatial distribution of laser's intensity is more concentrated and the peak intensity is higher for the influence of kinetic cooling of CO_2 and N_2; therefore, the efficiency of laser's irradiation is higher. It should be noted that the loss of energy propagation to the target is changeless for these three different conditions.

Figures 5 and 6 show the Strehl ratio and RMS of wavefront and peak intensity, respectively, on the target, which change with the original intensity launching from the laser system for two different conditions of the kinetic cooling on the last 2 km of propagation path and on the whole propagation link. It is observed that the beam quality and the efficiency of laser's irradiation on the dynamic target are more perfect when the kinetic cooling of atmosphere is considered. The consideration of kinetic cooling effect of atmosphere makes the evaluation of interaction efficiency of laser and target clearer.

The peak intensity of laser is 1000 W/cm² and the kinetic cooling of CO_2 and N_2 is considered on the whole propagation link.

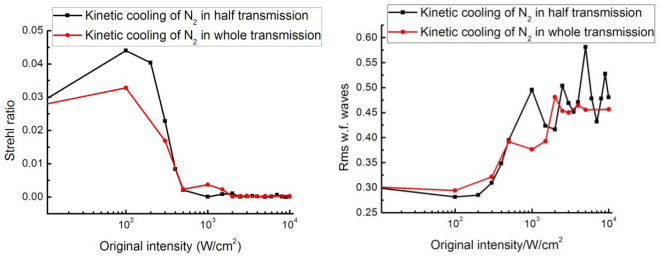

(a) (b)

Fig. 5. (a) Strehl's ratio and (b) RMS of wavefront for the kinetic cooling on the last 2 km of propagation path and on the whole propagation link.

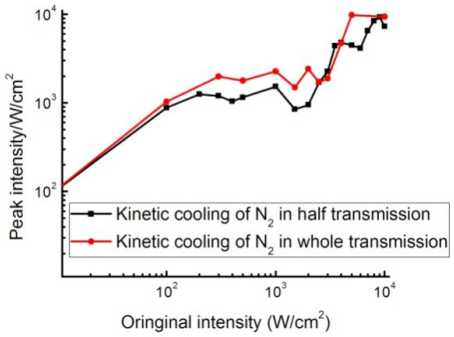

Fig. 6. Peak intensity on the target for the kinetic cooling on the last 2 km of propagation path and on the whole propagation link.

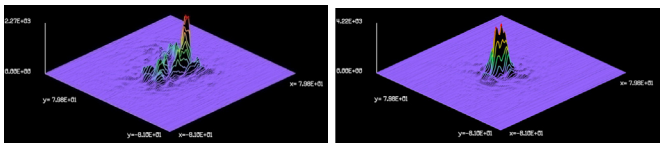

(a) (b)

Fig. 7. Spatial distribution of laser's intensity on the target for different speeds of target of (a) 3 and (b) 50 m/s.

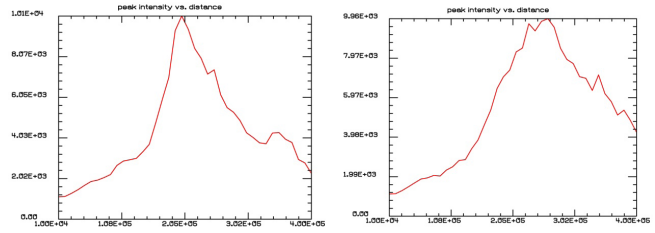

(a) (b)

Fig. 8. Peak intensity and real focus of laser on the optical propagation link for different speeds of target of (a) 3 and (b) 50 m/s.

Figures 7 and 8 show the spatial distribution of laser's intensity propagation to the flying target for different speeds of target. It is observed that the higher speed of target corresponds to better beam quality and higher peak intensity of laser propagation to the target. The spatial distribution of intensity on the target is more perfect to close to the ideal distribution of laser at far field when the speed of target comes to 330 m/s.

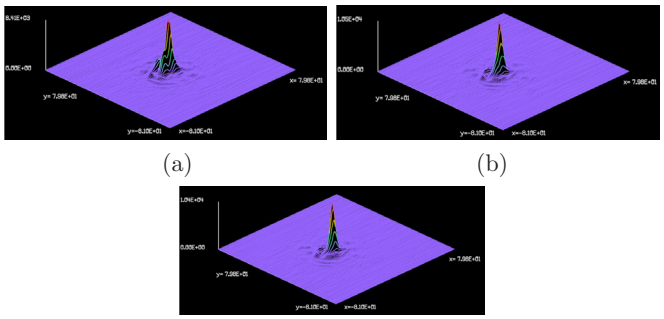

(a) (b) (c)

Fig. 9. Spatial distribution of laser's intensity on the target for different speeds of target of (a) 100, (b) 330, and (c) 1000 m/s.

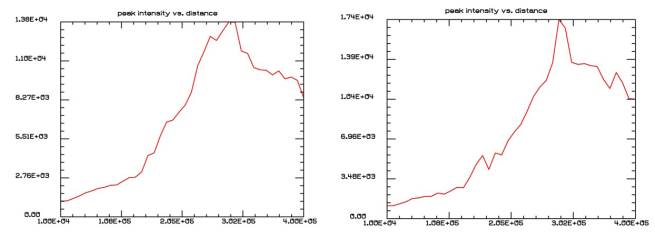

(a) (b)

Fig. 10. Peak intensity and real focus of laser on the optical propagation link for different speeds of target of (a) 100 and (b) 1000 m/s.

Figures 9 and 10 show the peak intensity and real focus of laser on the optical propagation link for different speeds of target. It is observed that the peak intensity is higher for higher speed of target and the real focus is closer to the geometric focus for the higher speed of target. As explained above, the higher speed of target influences the net speed v_c and changes ΔT, which is decided by thermal blooming of atmosphere. The influenced thermal blooming on the propagation link would change the refractive coefficient and change the real focus of the high power laser, therefore, the efficiency of laser's irradiation is improved.

Figures 11 and 12 show the Strehl ratio and RMS of wavefront and peak intensity, respectively, of laser irradiation on the flying target. It is observed that the beam quality and efficiency of laser's irradiation come to steady state and do not improve remarkably when the speed of target is higher than 330 m/s, as 330 m/s is the speed of expanding air for thermal blooming of atmosphere; therefore, the optical link balances slightly when the speed of target reaches the sonic speed and the ground to airspace system works well.

The peak intensity of laser is 1000 W/cm^2 and the kinetic cooling of CO_2 and N_2 is considered on the whole propagation link. The speed of target is 100 m/s.

Figures 13 and 14 show power distribution and spatial distribution of laser's intensity at near field on the target, the peak intensity and real focus of laser on the optical propagation link for different speeds of wind. It is observed that the higher speed of wind improves the beam quality and efficiency of laser's irradiation

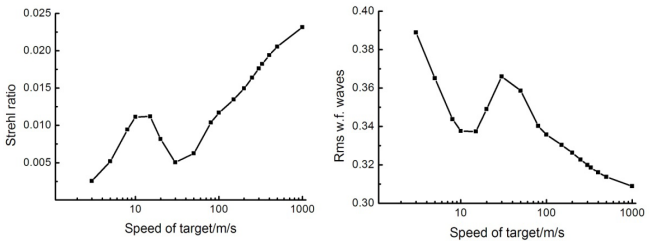

(a) (b)

Fig. 11. Strehl's ratio and RMS of wavefront for different speeds of target.

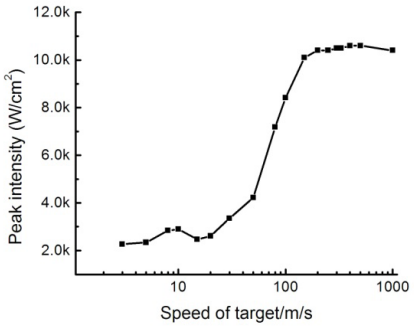

Fig. 12. Peak intensity of laser irradiation on the target for different speeds of target.

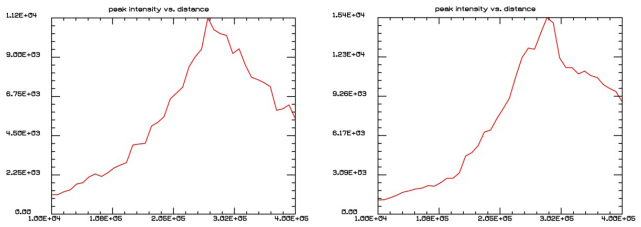

(a) (b)

Fig. 13. Power distribution for different speeds of wind of (a) 1 and (b) 15 m/s.

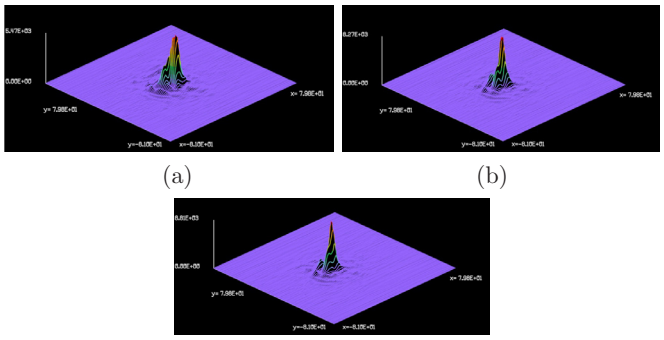

(a) (b)

(c)

Fig. 14. Spatial distribution of laser's intensity on the target for different speeds of wind of (a) 1, (b) 7, and (c) 15 m/s.

on the target. The real focus is closer to geometric focus for higher speed of wind. These perfect results are explained Eqs. (3) to (6). The higher speed of wind influences the net speed v_c and changes ΔT, which is decided by thermal blooming of atmosphere. The influenced thermal blooming on the propagation link changes the refractive coefficient and the real focus of the high power laser; therefore, the efficiency of laser's irradiation is improved.

Figures 15 and 16 show the Strehl ratio and RMS of wavefront and peak intensity, respectively, of laser propagation to the flying target. It is observed that the higher speed of wind corresponds to higher beam quality and more concentrated energy on the target, which means the higher efficiency of laser's irradiation.

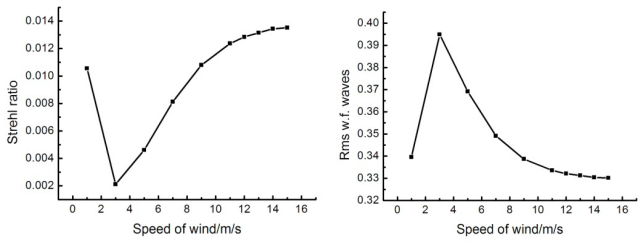

(a) (b)

Fig. 15. Strehl's ratio and RMS of wavefront for different speeds of wind.

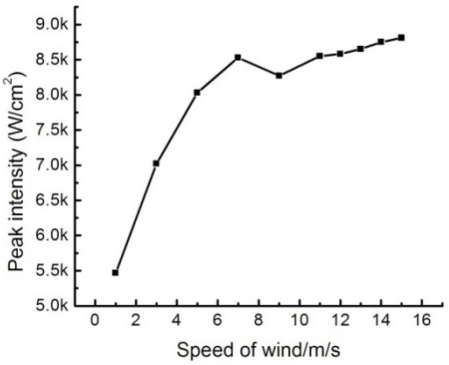

Fig. 16. Peak intensity of laser irradiation on the target for different speeds of wind.

For complicated atmospheric aberration, the direction of wind changes on the optical propagation link. The change in the direction of wind weakens the atmospheric aberration and improves the beam quality, which correspond to higher Strehl's ratio, lower RMS of wavefront and higher laser intensity irradiation on the dynamic target. Figures 17 and 18 show the contrast of two different conditions. It is observed that the simulation results are in agreement with the theory. Changes in the direction of wind improve the efficiency of laser's irradiation.

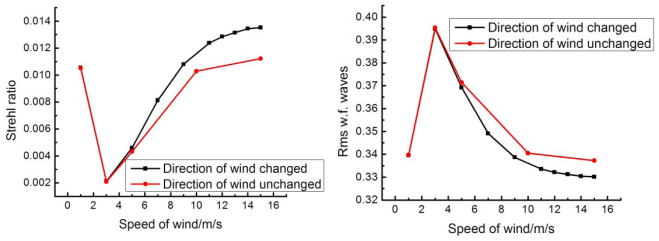

(a) (b)

Fig. 17. Strehl's ratio and RMS of wavefront for different speeds of wind when the direction of wind changes.

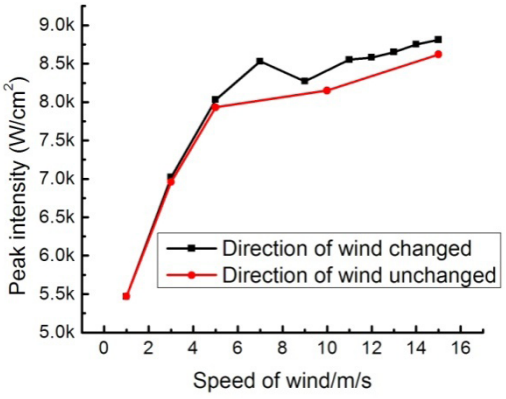

Fig. 18. Peak intensity for different speeds of wind when the direction of wind changes.

In conclusion, we simulate integrated effects of atmospheric aberration, atmospheric turbulence, thermal blooming, random jitter of laser's intensity and phase, speed of wind, direction of wind, absorption of air, kinetic cooling of CO_2 and N_2, speed of target, output power and beam quality of laser, wavelength, focus length and the launch altitude of laser to accurately simulate the transmission loss of the laser's energy, concentration of laser's power and other beam quality parameters of the laser propagating to the dynamic target, and we evaluate the efficiency of laser's irradiation on the target more accurately for the optical link of ground-to-airspace. We investigate the influences of characteristics of dynamic parameters (Strehl's ratio, RMS of wavefront, spatial distribution of intensity on the target, the real focus on the optical link and the peak intensity along the propagation path) including speed of wind, direction of wind, speed of target and the kinetic cooling effect of air, especially. We conclude that the higher speed of wind and target weakens the thermal blooming of atmosphere and improves the beam quality and efficiency of laser's irradiation on the target. The kinetic cooling effect of air is more remarkable to improve the beam quality irradiating on the target at the initial part of the propagation path of the laser. The change in the direction of the wind weakens the atmospheric aberration and results in better beam quality and higher efficiency of laser's irradiation on the target.

References

1. S. Gibson, "Atmospheric propagation of high energy lasers: modeling, simulation, tracking and control," AFOSR Grant F49620-02-01-0319 (Mechanical and Aerospace Engineering University of California, Los Angeles, 2008), p. 4.
2. W. He, "Simulation study on laser propagation through the atmospheric in optoelectronic countermeasures," PhD. Thesis (University of Electronic Science and Technology, 2012).
3. L. Ma, "Numerical simulation of Interaction between high energy laser and flying target," PhD. Thesis (National University of Defense Technology, 2006), p. 12.
4. R. Yang, "Research on several electromagnetic (optical) wave propagation problems on earth-space paths in troposphere atmosphere," PhD. Thesis (Xidian University, 2003), p. 5.
5. Z. He, "Analysis and design of Laser-propulsion lightcraft's configuration and ground based laser-propulsion launching mission," PhD. Thesis (National University of Defense Technology, 2008), p. 12.
6. D. C. Smith, "Investigation of self-induced thermal effects of CO_2 laser irradiation propagating in absorbing gases," United Aircraft Research Laboratories East Hartford, Connecticut, AD-765 520 (for CO_2) (United Aircraft Research Laboratories East Hartford, Connecticut, 1972).
7. www.aor.com, "GLAD Theory Manual ver.5.5," Applied Optics Research (1087 Lewis River Rd. #217, Woodland, WA 98674, 2009), p.259